

Directivity Correction of Seismic Data for Improved AVO Analysis of Bottom Simulating Reflector

Debasis Chaudhuri*, Dr. Achintya Pal, P K Chaudhuri & A V Sathe

ONGC, Dehradun

Summary

Bottom Simulating Reflector (BSR) is the only indirect evidence of gas hydrate accumulation seen in seismic data along with associated features like amplitude blanking etc. On CDP gathers, BSR horizon evinces a classic class III AVO effect where absolute amplitude increases with offset. Although the class III AVO in the case of BSR is not always indicative of gas, however this characteristic of BSR as well as many horizons with underlying gas pool has been a hot (bright?) spot of research in seismic industry. In the case of class III AVO, the angle dependent reflectivity increases the amplitude with offset. But due to angle dependent directivity factor, the loss of amplitude with offset smudges the true increase of amplitude with offset. The so called "True Amplitude Recovery" does not address this factor. Due to this reason, occurrences of class III AVO may escape detection and elude exploration effort. On AVO analysis of directivity corrected gathers, the gradient is restored and hence shows true scattering on the P-G crossplot. Here an attempt has been made to first extract the directivity factor by analyzing the observed amplitude of seabed reflection and comparing it with an a-priori model of the seafloor. The directivity factor is then applied to the CDP gathers to compensate for the loss of amplitude with angle. The directivity corrected gathers are inverted to extract the AVO intercept and gradient and the P-G crossplot is compared with that of the original data to show improved scatters. The data is from a 2D seismic line from Krishna Godavari basin of east coast of India which is a proven oil & gas field and evinces excellent BSR. *In this paper the polarity of the data is trough for a compression i.e. seafloor is a trough and BSR is a peak.*

Introduction

Gas hydrates are ice like crystals formed due to encasement of primarily methane gas in hydrogen bonded water lattices. The formation of methane hydrates requires high pressure and low temperature. All over the world, in permafrost area and in continental slope area with deeper bathymetry these conditions prevail and gas hydrates may form depending upon availability of gas. Gas hydrates have great entrapment capability and on dissociation 1 cum. of pure gas hydrates release 164 cum. of gas at STP and 0.8 cum of pure water. Kvenvolden first made an estimate of gas hydrate resources for the world and it turned out to be 20000 TCM which is more than double the carbon content of the total fossil fuel reserve of the world. Many energy starved and techno-savvy countries have put in a lot of money and effort in order to explore and exploit this giant resource.

In India, gas hydrates form in the deep continental slope region where the bathymetry exceeds 650 to 700 m (Chaudhuri, 2002). The entire deep continental slope of Indian waters is prone to gas hydrate formation due to favorable pressure and temperature condition (Chaudhuri, 2003). The Seismic data from the entire Indian offshore were scanned for BSR signature. Based on this investigation,

Krishna-Godavari (K-G) offshore and Andaman offshore in the east coast of India were found to be most prospective for gas hydrate exploration (Rao, 2003 & 2004).

In multi-channel seismic data, on pre-stack CDP gathers the amplitude varies with offset due to (a) decay of amplitude with spherical divergence and directivity, (b) absorption of energy in sediments and (c) the angle dependent nature of reflectivity. The true geological effect is buried in the last component(c) which however can be masked by the first two factors (a) & (b). In the case of class III AVO the increase in amplitude with offset is not always discernable due to this fact. But if by applying directivity correction, the loss in amplitude due to directivity can be compensated for while keeping the angle dependent reflectivity intact, the suppressed AVO effect can be accentuated resulting in effective delineation of a prospect. In the present work, a part of seismic section from KG offshore is selected (Fig. 1) and directivity correction is applied. The data is inverted for extraction of AVO intercept and gradient. The AVO gradient is much more pronounced after the directivity correction. The P-G crossplots before and after the directivity correction show improved scattering indicating anomalies below the BSR.

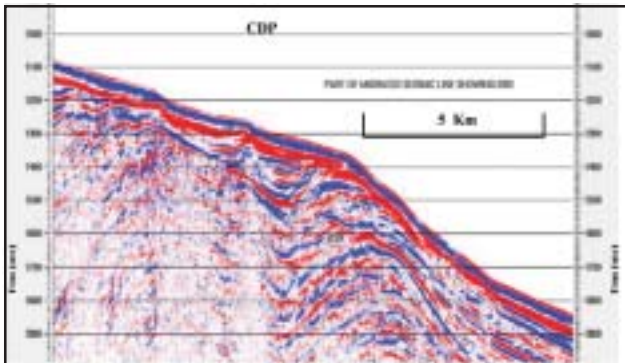


Fig. 1 : Section from Indian deep water showing BSR

Theory

For a spiked impulse, the amplitude on a CDP gather of MCS data can be represented as:

$$A(\theta) = R(\theta) \times D(\theta) \dots \dots \dots (1)$$

where,

- A(θ) = Composite amplitude at an incident angle θ.
- R(θ) = Amplitude due to reflectivity at an incident angle θ.
- D(θ) = Directivity factor at an incident angle θ.

The directivity factor arises due to two reasons. The air-gun array is designed so as to obtain the maximum primary to bubble ratio in the vertical direction. This gives rise to a variation in input strength of the composite pulse with angle. The second factor of directivity comes from the angle dependence of the receiver response. With increasing θ, D(θ) decreases resulting in amplitude decay with offset. This is quite independent of R(θ) which changes with angle depending on several physical parameters of the overlying and underlying medium.

From (1), we can write

$$D(\theta) = A(\theta) / R(\theta) \dots \dots \dots (2).$$

The R(θ) component is calculated by modeling the p-p reflection coefficient for isotropic medium using complete wave equation with stress free boundary condition at the sea surface (Mallick,1991).

The model reflection coefficient is used to calculate D(θ) from the seismogram. A least square fit is applied to the D(θ) values to extract the decay vs. angle curve. The inverse of this curve gives the compensation vs. angle curve which is multiplied with the A(θ) values to obtain the directivity corrected seismogram.

Results & discussion

Fig 1 shows a seismic line showing a prominent BSR approximately 200 ms. below the seafloor. A part of this line (100 CDP) is taken for directivity correction. On modeling, the seafloor shows a class I AVO whereas the BSR shows a class III AVO response at large offsets (Fig. 2) However on a closer inspection, the BSR model shows a decrease in absolute amplitude up to an angle of 16 deg. and then starts increasing again (Fig. 3). Incidentally, this type of AVO response is not classified in any literature (Roger, 2003).

The decrease in amplitude with angle due to directivity at the sea floor and the corresponding correction is shown in fig. 5. The AVO gradient (Fig. 6) shows an appreciable increase in amplitude after directivity correction when compared to the original data. The AVO gradient is calculated at one CDP by picking the highest amplitude within a gate for both normal and directivity corrected data (Fig. 7). The gradient shows an improvement from -0.33 to -1.98.

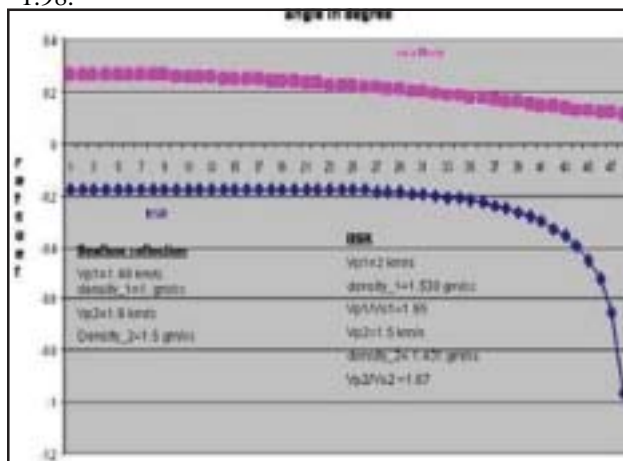


Fig.2 : Modeled seafloor and BSR

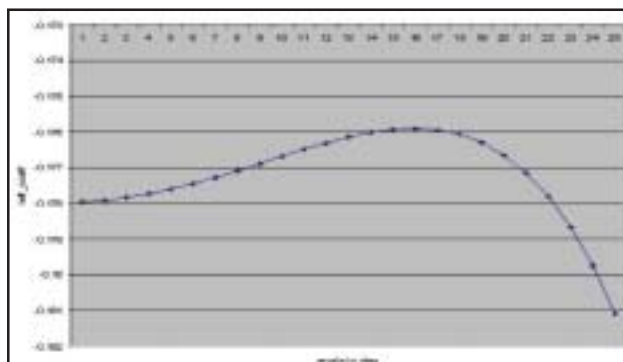


Fig.3 : Close-up of modeled BSR

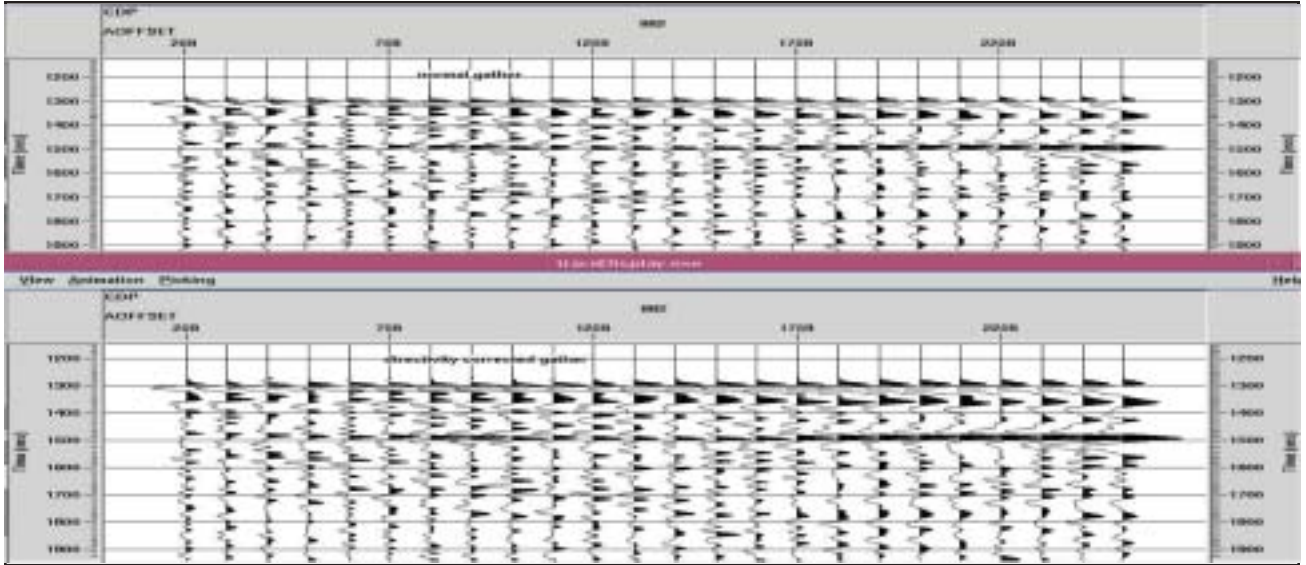


Fig.4 : Comparison of normal and directivity corrected Gather. (Top- normal; bottom- directivity corrected.)

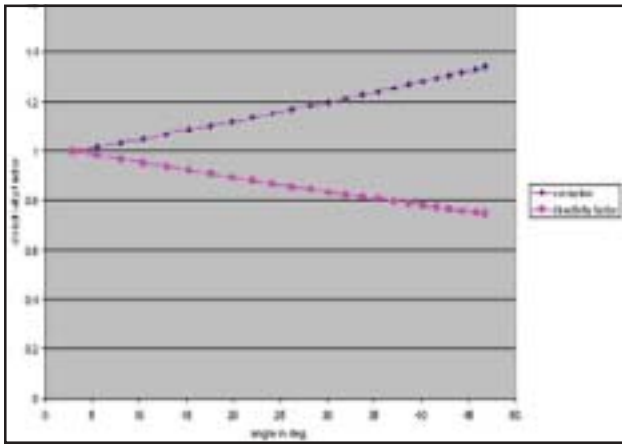


Fig. 5 : Loss due to directivity & its correction

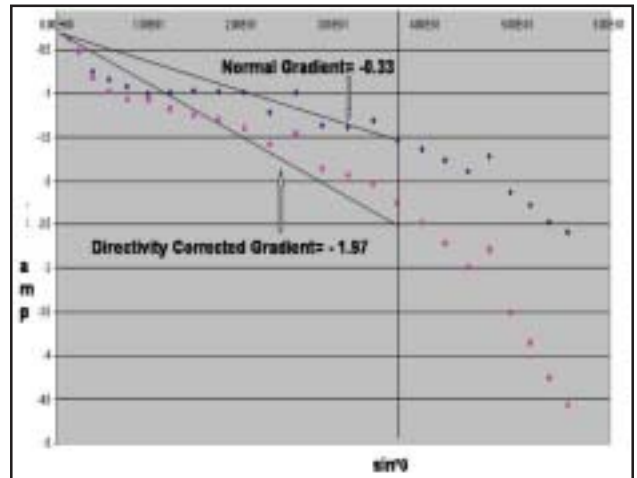


Fig.7 : AVO gradient before and after correction at one CDP.

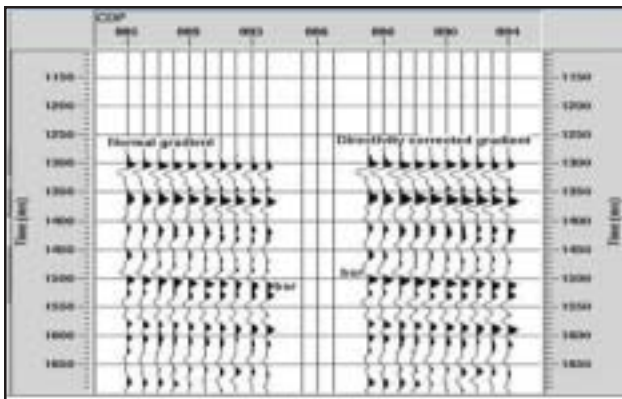


Fig.6 : AVO gradient before and after directivity correction

The corresponding stack section (Fig. 8) also shows improvement on the directivity corrected stack as compared to the original stack. P-G crossplots are generated for both the data sets from a 100 ms window with BSR horizon at the centre. Fig. 9 shows the P-G crossplot for the original data whereas Fig. 10 shows the same for the directivity corrected data. On comparison, although the basic scattering pattern is same in both the plots, Fig.10 shows more pronounced anomalies.

Although the present results are limited to the AVO attributes of a BSR which shows a class III AVO response,

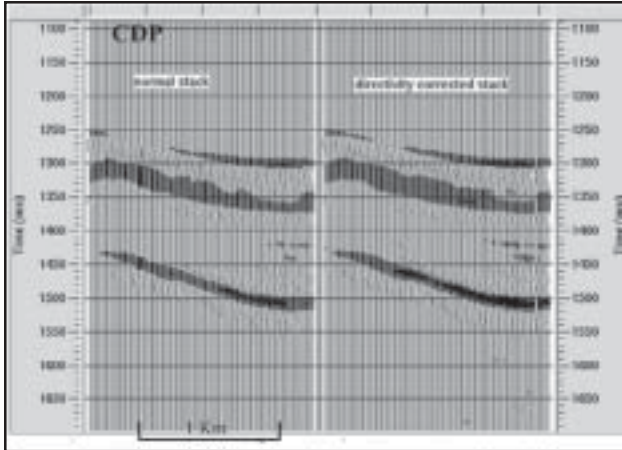


Fig.8 : Comparison of normal and directivity corrected stacks (L- normal; R- directivity corrected)

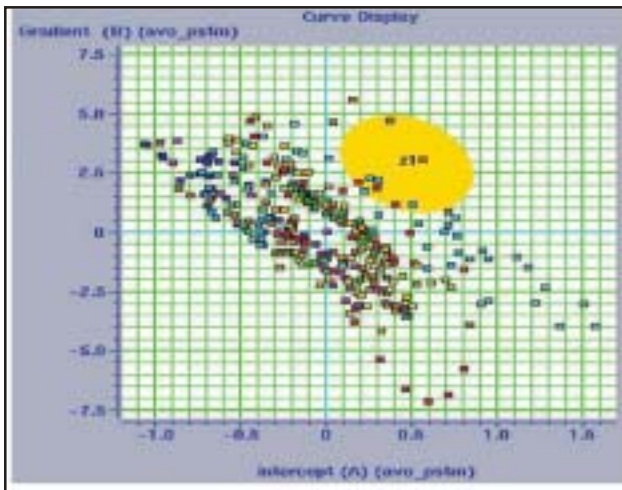


Fig. 9 : P-G crossplot without directivity correction

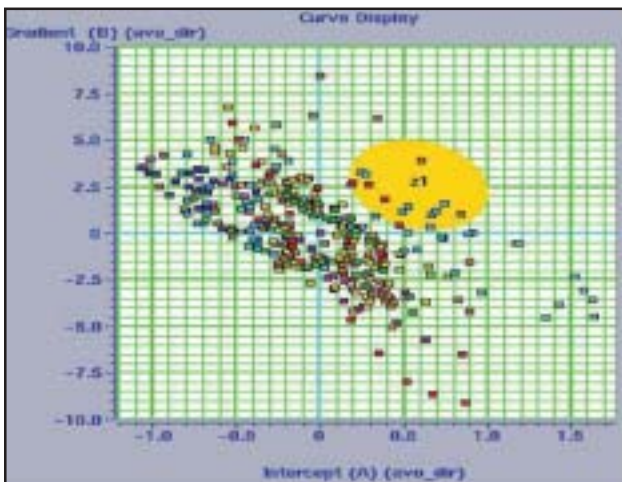


Fig. 10 : P-G crossplot with directivity correction. The anomaly is appreciably separated due to improved scatter.

this methodology can be extended where the reflector does not show any AVO on normal gathers, but geological intuition foretells the presence of anomaly. Here, P-G crossplot of directivity corrected datasets may bring out the subtle anomalies which otherwise elude inspection and subsequent investigation.

Disclaimer

The views expressed in this paper are of the authors only and not necessarily those of the organizations they are working for.

Acknowledgement

The authors are grateful to the Director (Exploration) for according permission to present the work. We are indebted to Dr. D. Ray, ED – Head KDMIPE and D. Sar, GM (Geophysics) for guidance and encouragements.

References

- Chaudhuri D., Chandra S. and Sathe A.V., 2003, Gas hydrates, inversion and AVO, Proceedings of PETROTECH-2003.
- Chaudhuri, D., Lohani N. C., Chandra S. and Sathe A.V., 2002, AVO attributes of a Bottom Simulating Reflector: east coast of India, 72nd SEG Conference, Salt Lake City, Utah, USA.
- Chaudhuri, D., Sathe A.V., Chandra,S. and Varughese C. M., 2002 , Exploitation of gas hydrate- A concept. 4th SPG Conference, Mumbai, India.
- Rao C.M., Chaudhuri D., P. K. Saha, 2003 & 2004, “ Gas Hydrate Studies in Indian offshore”, unpublished reports of KDMIPE, ONGC, Dehradun.
- Roger A Young, Robert D LoPiccolo, Oct’2003,” A comprehensive AVO classification”, The Leading Edge.
- Mallick S., and Frazer L.N., 1991, Reflection/transmission coefficients and azimuthal anisotropy in marine seismic studies, Geophysical. Journal. International, **105**, 241-252.